VLBI Analyses using Covariance Information from Turbulence Models

Sebastian Halsig, Thomas Artz, Judith Leek, Axel Nothnagel

Abstract Refractivity variations in the troposphere represent a dominant contribution to the error budget of the observations of Very Long Baseline Interferometry (VLBI). In fact, they limit the accuracy of the VLBI target parameters. These refractivity variations also lead to elevation-dependent uncertainties and affect the correlations between observations. However, such stochastic properties are generally not considered in VLBI data analysis leading to deficiencies in modeling the stochastic properties of the observations. Thus, formal errors are generally too optimistic.
In this study, the stochastic model is modified. The standard stochastic information from the VLBI correlation process is now augmented by the variance-covariance information derived from atmospheric turbulence models based on the Kolmogorov turbulence theory. Thus, we obtain a fully populated variance-covariance matrix of observations, which is incorporated in the VLBI analysis. In order to validate our results, this approach will be applied to the continuous VLBI campaign 2011 (CONT11).

Keywords VLBI, stochastic properties, refractivity variations, Kolmogorov turbulence theory, turbulence model

1 Introduction

The observations of space-geodetic techniques, such as Very Long Baseline Interferometry (VLBI) or Global Navigation Satellite Systems (GNSS), are affected by refractivity variations in the neutral atmosphere. Today, only long-periodic variations are considered routinely. Micro-scale meteorological phenomena are not taken into account, limiting the attainable accuracy of the VLBI target parameters.

In general, the total tropospheric delay can be modeled by a hydrostatic (index h) and a wet (index w) component [3]. Each of these terms consists of a zenith delay (ΔL_h^z and ΔL_w^z) and a corresponding mapping function ($mf_h(\varepsilon)$ and $mf_w(\varepsilon)$) for the transformation from zenith to an arbitrary elevation angle ε,

$$\Delta L(\varepsilon) = mf_h(\varepsilon)\Delta L_h^z + mf_w(\varepsilon)\Delta L_w^z. \qquad (1)$$

The hydrostatic delay on the one hand mainly depends on the air pressure and is generally taken into account by using surface pressure measurements and applying an adequate model [3]. Due to the high temporal and spatial variability of water vapor in the atmosphere, the variations of the wet component on the other hand are unpredictable. Thus, the zenith wet delay is estimated as an additional correction parameter within the VLBI estimation process.

Dynamic processes in the atmosphere, particularly refractivity fluctuations, also lead to elevation-dependent uncertainties and induce physical correlations between observations. However, the stochastic model in the VLBI analysis only includes uncertainties from the VLBI correlation process [14]. Other error sources, such as remaining correlator related errors, uncertainties in the phase calibration, source position and structure errors, deficits in modeling the station coordinates or model errors (e.g., atmosphere, clocks), are not modeled in the VLBI standard approach. Thus, the variance-covariance matrix (VCM) in the VLBI analysis is only sparsely populated and formal errors

Institute of Geodesy and Geoinformation, University of Bonn

for the derived parameters, such as station coordinates, and Earth orientation parameters, are too optimistic. An indication for the fact that other noise sources should be taken into account and that there are deficiencies in the current stochastic modeling is given by the χ^2 statistics, i.e., $\chi^2 = \frac{\sigma_0^2}{\hat{\sigma}^2}$, where σ_0^2 and $\hat{\sigma}^2$ denote the a priori and a posteriori variance, respectively. Regarding χ^2 values from individual session solutions, they are in general much larger than they should be [4]. The standard approach in Calc/Solve is to re-weight the observations by iteratively adding additional noise until $\chi^2 \approx 1$.

Earlier studies have been carried out to investigate the stochastic properties of VLBI observations. For instance, Tesmer and Kutterer [11] refined the traditional stochastic model by means of expending the variances of the observations by source-, station-, and elevation-dependent components. Gipson et al. [4] included station-dependent noise in the VLBI analysis which leads to an increase of the observational noise. Romero-Wolf et al. [8] presented a simplified application of the turbulence-based stochastic model for tropospheric delays developed by Treuhaft and Lanyi [12] to a set of VLBA catalog runs. Nilsson and Haas [6] used simulations of atmospheric delays to validate the impact of atmospheric turbulences on VLBI observations during the continuous VLBI campaigns CONT05 and CONT08.

This contribution extends the existing approaches by an external way to model physical correlations due to refractivity variations in the neutral atmosphere. For this purpose, the more general atmospheric turbulence model of Schön and Brunner [9] is used to obtain a fully populated variance-covariance matrix of the observations which is incorporated in the VLBI analysis in a second step. This leads to a more adequate modeling of the stochastic properties in the VLBI analysis.

2 Modeling Atmospheric Turbulence

Atmospheric turbulence can be best described stochastically following the widely accepted turbulence theory of Kolmogorov. In turbulence theory, the stochastic properties are usually described by the so-called structure function that contains information of scatter and statistical covariance. An integration of the structure function of refractivity along the line-of-sight (LOS) leads to a VCM of the tropospheric delays (for more detail see, e.g., [6, 12]).

As an alternative approach, Schön and Brunner developed a turbulence model [9] for GPS carrier phase data, based on a 3D spectrum representation. Since restrictive conditions, such as inhomogeneity and anisotropy, can be taken into account, this approach leads to a more general description of the VCM in comparison to the structure function expression [9].

Since the initial formulation of the spectral representation by Kolmogorov has a singularity for $\kappa = 0$, the 3D spectrum Φ_n for refractivity fluctuations is expressed by the van Karman spectrum [13],

$$\Phi_n(\kappa) = \frac{0.033 C_n^2}{\left(\kappa^2 + \kappa_0^2\right)^{\frac{11}{6}}} \sim \kappa^{\frac{-11}{3}}, \qquad 0 < \kappa < \kappa_s. \quad (2)$$

Here, C_n^2 denotes the structure constant of refractivity which, roughly speaking, expresses the strength of turbulence. κ represents the wave numbers with κ_0 and κ_s being the wave numbers corresponding to the outer and inner scale length, respectively [13].

Integrating the refractivity variations along the line-of-sight, the spectrum of refractivity, which can be best described by the Fourier wave number decomposition, can be related to the covariances of the tropospheric delay [9],

$$\left\langle \tau_A^i(t_A), \tau_B^j(t_B) \right\rangle = \int_0^\infty \int_0^\infty \int_{-\infty}^\infty \int_{-\infty}^\infty \int_{-\infty}^\infty \Phi_n\left(\hat{\kappa}, \frac{\mathbf{r}_A^i + \mathbf{r}_B^j}{2}\right) e^{i\hat{\kappa}^T \mathbf{d}} \mathbf{d}^3 \hat{\kappa} ds_1 ds_2. \quad (3)$$

Here, $\mathbf{r}_A^i$, $\mathbf{r}_B^j$ are the LOS vectors between station A and source i, and station B and source j, respectively. Please note that for a more specific VLBI configuration two stations (A and B) and only one source ($i = j$) are used. The 3D vector of wave numbers is denoted by $\hat{\kappa}$,

$$\mathbf{d} = \mathbf{r}_B^j(ds_2) + \varphi_A^B - \mathbf{v}\Delta t - \mathbf{r}_A^i(ds_1), \quad (4)$$

represents the vector separating the integration points and φ_A^B denotes the baseline.

Besides the spatial correlations, temporal correlations are taken into account using Taylor's frozen flow model [13]. It is assumed that the turbulent medium is frozen during the observation time and travels in wind direction with a constant velocity $v > 0$. The temporal

separation Δt is multiplied with the constant wind vector $\mathbf{v}$. Thus, the temporal separation is transformed to a spatial separation and can be added to Equation 4.

After a few modifications (for more details, see [9]) and transforming the integration over the slant direction to an integration over the zenith direction ($dz_i = \sin\varepsilon_i ds_i$) yields the following expression for the covariances of the tropospheric delays,

$$\left\langle \tau_A^i(t_A), \tau_B^j(t_B) \right\rangle = \frac{12}{5}\frac{0.033}{\Gamma\left(\frac{5}{6}\right)}\frac{\sqrt{\pi^3}\kappa_0^{-\frac{2}{3}}2^{-\frac{1}{3}}}{\sin\varepsilon_A^1 \sin\varepsilon_B^2}C_n^2 \cdot \int_0^H\int_0^H (\kappa_0 d)^{\frac{1}{3}} K_{-\frac{1}{3}}(\kappa_0 d)\, dz_1 dz_2, \tag{5}$$

where d represents the separation distance between the actual integration points [9], Γ denotes the gamma function [1] and K is the modified Bessel function of second kind [1]. Similarly, we receive a representation for the variances. Here, all expressions can be analytically integrated, yielding

$$\left\langle \tau^2 \right\rangle = \frac{12}{5}\frac{0.033}{\Gamma\left(\frac{5}{6}\right)}\frac{\sqrt{\pi^3}\kappa_0^{-\frac{2}{3}}2^{-\frac{1}{3}}}{(\sin\varepsilon)^2}C_n^2 H^2 \cdot \left\{ \frac{\pi 2^{\frac{1}{3}}}{\sqrt{3}\Gamma\left(\frac{2}{3}\right)} F_3^2\left(\left[\frac{1}{2},1\right],\left[\frac{2}{3},\frac{3}{2},1\right],\frac{z^2}{4}\right) - \frac{27}{80}2^{\frac{2}{3}}\Gamma\left(\frac{2}{3}\right) z^{\frac{2}{3}} F_2^1\left(\left[\frac{5}{6}\right],\left[\frac{11}{6},\frac{7}{3}\right],\frac{z^2}{4}\right)\right\}. \tag{6}$$

Here, F denotes the hypergeometric function [1] and it holds that $z = \frac{p\kappa_0 H}{\sin\varepsilon}$, where H is the effective tropospheric height and p describes the impact of anisotropy on the variance [9].

3 Analysis Setup

The atmospheric turbulence model is applied to the CONT11 campaign provided by the International VLBI Service for Geodesy and Astrometry (IVS, [10]). The databases are initially processed using the VLBI analysis software Calc/Solve [5], which was modified to export the normal equation system. A stand-alone C++ back-end to Calc/Solve is used to incorporate the additional variance-covariance matrix into the least-squares adjustment. The new ensemble variance-covariance matrix is the square sum of the weight matrix of the correlation process and the additional matrix from turbulence modeling. Then, the program is used to build and solve the normal equation system. The modeling and analysis setup described in [2] is used for all solutions.

4 Results

Different solution setups have been analyzed which differ primarily in the parametrization of the structure constant C_n^2, the effective tropospheric height H, and the wind vector $\mathbf{v}$ (cf. Table 1). In particular, the structure constant is either assumed to be equal for each station (setups 3 and 4) or estimated from radar measurements, radiosonde data or GNSS data (setups 5, 6, and 7). In the latter case, the station-dependent C_n^2 values are taken from [6] or [7]. Different methods for estimating C_n^2 are presented by Nilsson and Haas [6].

Table 1 Solution setups w.r.t. the Calc/Solve re-weighting option and the parametrization of the structure constant (equal for all stations or station-dependent estimates), the tropospheric effective height (equal for all stations or station-dependent estimates), and the wind vector. The mean χ^2 value [-] and WRMS post-fit residuals for the delay observables, converted to [mm], are given for the CONT11 interval.

	re-wt.	C_n^2	H	$\mathbf{v}$	χ^2	WRMS
1	+	-	-	-	0.83	25.07
2	-	-	-	-	3.68	26.32
3	-	C_n^2 = 1.0	1 km	8 $\frac{m}{s}$	3.25	17.22
4	-	C_n^2 = 1.0	2 km	8 $\frac{m}{s}$	2.99	16.50
5	-	est.,[7]	2 km	8 $\frac{m}{s}$	2.32	14.55
6	-	est., [6]	est., [6]	8 $\frac{m}{s}$	2.27	14.39
7	-	est.,[7]	2.5 km	8 $\frac{m}{s}$	2.17	14.01

To validate the different solutions, the χ^2 value (Figure 1) and the weighted root mean squared (WRMS) post-fit residuals of the delay observables are given in Figure 1 and Figure 2, respectively, for each day of the CONT11 campaign. The mean values over the CONT11 time period are shown in Table 1.

The χ^2 value is a criterion whether the global test for an adjustment is fulfilled or not, which would be the case if $\chi^2 \approx 1$. As expected, this is true for the standard Calc/Solve solution (black diamonds), because

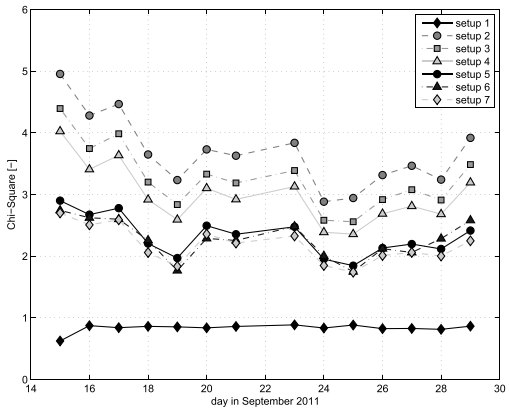

Fig. 1 Validation of the different solution parametrizations for the CONT11 campaign: χ^2 values [-].

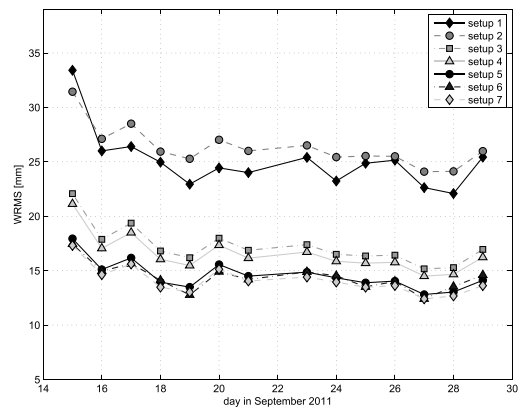

Fig. 2 Validation of the different solution parametrizations for the CONT11 campaign: weighted root mean squared (WRMS) post-fit residuals of the delay observables, converted to [mm].

additional noise is iteratively added to the observations as described above. Turning off the re-weighting option, typical values are $\chi^2 \approx 3-4$ [4], which is equal to our solution (setup 2, dark gray points). Compared to this reference value, the solutions with constant atmospheric parameters (setup 3, dark gray squares or setup 4, light gray triangles) lead only to a little decrease in the χ^2 value. Using estimated structure constants (setup 5, black circles; setup 6, black triangles, setup 7, light gray diamonds) leads to a reduction of the χ^2 value. However, the χ^2 values are still little too high for all cases.

For the same solution setup, Figure 2 shows the weighted root mean squared (WRMS) scatter per solution based on the post-fit residuals. It is obvious that for some solutions, particularly those using the more realistic C_n^2 values (setup 5, black circles; setup 6, black triangles; setup 7, light gray diamonds), the WRMS post-fit residuals decrease sharply compared to the reference solution defined above. There are only small differences in the three solution types using estimated C_n^2 values.

Besides the given statistics, the baseline length repeatabilities are calculated for a Calc/Solve solution re-weighting the observations (setup 1, black diamonds) and a least-squares adjustment with additional turbulence modeling (setup 3, dark gray squares). The results are shown in Figure 3(a). Both solutions are quite similar and the root mean squared (RMS) error for the baseline length repeatabilities decreases sharply compared to a solution without re-weighting (setup 2, dark gray points). Further, a quadratic polynomial is estimated for all baseline lengths. It should be noted here that for the different solution setups (2–7) only minor variations in the baseline length repeatabilities are observed (not shown here).

The RMS differences between the Calc/Solve solution re-weighting the observations and the solution concerning atmospheric conditions are presented in Figure 3(b). Whereas black bars indicate an improvement, light gray bars denote a degradation. In this comparison, about 25% of the baselines are improved by at least 1 mm, whereas 12% get worse by at least 1 mm and 63% remain unchained.

5 Conclusion and Future Work

The turbulence model developed by Schön and Brunner [9] is used to obtain information about the stochastic properties of tropospheric refractivity variations. The resulting VCM is added to the weights from the VLBI correlation process and the ensemble VCM is incorporated into the VLBI analysis. This approach has been applied to the CONT11 campaign for different solution types w.r.t. the structure constant, the tropospheric height, and the wind vector parametrization.

It was shown that the WRMS post-fit residuals decrease sharply when using estimated C_n^2 values, e.g., from GNSS estimation. The baseline length repeatabilities improve slightly, but only minor variations between the different solution setups are observed. Al-

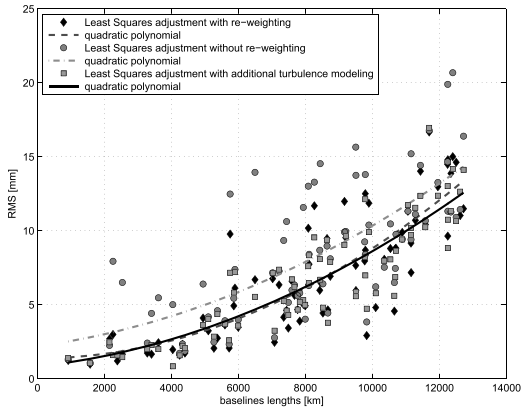

(a)

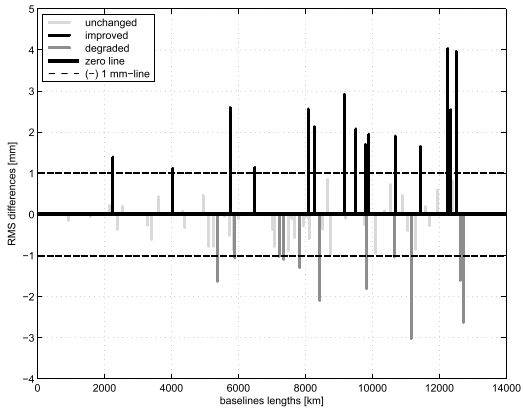

(b)

Fig. 3 Baseline length repeatabilities (a) for a least-squares adjustment with (setup 1, black diamonds) and without (setup 2, dark gray points) re-weighting the observations as well as for a least-squares adjustment with turbulence modeling (setup 3, dark gray squares). RMS differences (b) between setup 1 and 3. Black bars show an improvement, dark gray bars denote a degradation and light gray bars indicate unchanged baseline lengths.

though the χ^2 values decrease for the new approach, they are still a little too high indicating that the observational noise is still underestimated or that there are some other terms that are not adequately modeled.

In a next step, special consideration should be given to the parametrization of the wind velocity and direction that is assumed to be constant in this study. Further, and even more important, other error sources—e.g., source position and structure errors, remaining correlator related errors, uncertainties in phase calibration, or further model errors—have to be investigated and modeled adequately as well.

Acknowledgements

The authors thank the German Research Foundation (Deutsche Forschungsgemeinschaft, DFG) for its financial support (contract NO 318/10-1).

References

1. M. Abramowitz and I. A. Segun. Handbook of mathematical functions. *Dover Publications*, New York, 1972
2. T. Artz, S. Böckmann, A. Nothnagel, P. Steigenberger. Subdiurnal variations in the Earth's rotation from continuous Very Long Baseline Interferometry campaigns. *J Geophys Res*, 115, B05404, doi: 10.1029/2009JB006834, 2010
3. J. L. Davis, T. A. Herring, I. I. Shapiro, A. E. E. Rogers, G. Elgered. Geodesy by radio interferometry: Effects of atmospheric modeling errors on estimates of baseline length. *Radio Sci*, 20(6), pp. 1593–1607, 1985
4. J. Gipson, D. MacMillan, L. Petrov. Improved Estimation in VLBI through Better Modeling and Analysis. *IVS 2008 General Meeting Proc.*, pp. 157–162, 2008
5. C. Ma, J. M. Sauber, T. A. Clark, J. W. Ryan, L. J. Bell, D. Gordon, W. E. Himwich. Measurement of horizontal motions in Alaska using very long baseline interferometry. *J Geophys Res*, 95(B13), doi: 10.1029/JB095iB13p21991, 1990
6. T. Nilsson and R. Haas. Impact of atmospheric turbulence on geodetic very long baseline interferometry. *J Geophys Res*, 115, B03407, doi: 10.1029/2009JB006579, 2010
7. T. Nilsson, R. Heinkelmann, M. Karbon, V. Raposo-Pulido, B. Soja, H. Schuh. Earth orientation parameters estimated from VLBI during the CONT11 campaign. *J Geodesy*, 88, doi: 10.1007/s00190-014-0700-5, pp. 491–502, 2014
8. A. Romero-Wolf, C. S. Jacobs, J.T. Ratcliff. Effects of Tropospheric Spatio-temporal Correlated Noise on the Analysis of Space Geodetic Data. *IVS 2012 General Meeting Proc.*, pp. 231–235, 2012
9. S. Schön and F. K. Brunner. Atmospheric turbulence theory applied to GPS carrier-phase data. *J Geodesy*, 82, doi: 10.1007/s00190-007-0156-y, pp. 47–57, 2008
10. H. Schuh and D. Behrend. VLBI: A fascinating technique for geodesy and astrometry. *Journal of Geodynamics*, 61, doi: 10.1016/j.jog.2012.07.007, pp. 68–80, 2012
11. V. Tesmer and H. Kutterer. An advanced Stochastic Model for VLBI Observations and its Applications to VLBI Data Analysis. *IVS 2004 General Meeting Proc.*, pp. 296–300, 2004
12. R. N. Treuhaft and G. E. Lanyi. The effect of the dynamic wet troposphere on radio interferometric measurements. *Radio Sci*, 22(2), pp. 251–265, 1987
13. A. D. Wheelon. Electromagnetic Scintillation - I. Geometrical Optics. *Cambridge University Press*, Cambridge, 2004
14. A. Whitney. How Do VLBI Correlators Work? *IVS 2000 General Meeting Proc.*, pp. 187–205, 2000